Biogeosciences, 7, 2695–2709, 2010
www.biogeosciences.net/7/2695/2010/
doi:10.5194/bg-7-2695-2010

Biogeosciences

Biogeochemical controls and isotopic signatures of nitrous oxide production by a marine ammonia-oxidizing bacterium

C. H. Frame[1,2] **and K. L. Casciotti**[1]

[1]Marine Chemistry and Geochemistry, Woods Hole Oceanographic Institution, Woods Hole, Massachusetts, USA
[2]Joint Program in Chemical Oceanography, MIT Woods Hole Oceanographic Institution, Woods Hole, Massachusetts, USA

Received: 2 April 2010 – Published in Biogeosciences Discuss.: 27 April 2010
Revised: 30 July 2010 – Accepted: 10 August 2010 – Published: 13 September 2010

Abstract. Nitrous oxide (N_2O) is a trace gas that contributes to the greenhouse effect and stratospheric ozone depletion. The N_2O yield from nitrification (moles N_2O-N produced per mole ammonium-N consumed) has been used to estimate marine N_2O production rates from measured nitrification rates and global estimates of oceanic export production. However, the N_2O yield from nitrification is not constant. Previous culture-based measurements indicate that N_2O yield increases as oxygen (O_2) concentration decreases and as nitrite (NO_2^-) concentration increases. Here, we have measured yields of N_2O from cultures of the marine β-proteobacterium *Nitrosomonas marina* C-113a as they grew on low-ammonium (50 µM) media. These yields, which were typically between 4×10^{-4} and 7×10^{-4} for cultures with cell densities between 2×10^2 and 2.1×10^4 cells ml^{-1}, were lower than previous reports for ammonia-oxidizing bacteria. The observed impact of O_2 concentration on yield was also smaller than previously reported under all conditions except at high starting cell densities (1.5×10^6 cells ml^{-1}), where 160-fold higher yields were observed at 0.5% O_2 (5.1 µM dissolved O_2) compared with 20% O_2 (203 µM dissolved O_2). At lower cell densities (2×10^2 and 2.1×10^4 cells ml^{-1}), cultures grown under 0.5% O_2 had yields that were only 1.25- to 1.73-fold higher than cultures grown under 20% O_2. Thus, previously reported many-fold increases in N_2O yield with dropping O_2 could be reproduced only at cell densities that far exceeded those of ammonia oxidizers in the ocean. The presence of excess NO_2^- (up to 1 mM) in the growth medium also increased N_2O yields by an average of 70% to 87% depending on O_2 concentration. We made stable isotopic measurements on N_2O from these cultures to identify the biochemical mechanisms behind variations in N_2O yield. Based on measurements of $\delta^{15}N^{bulk}$, site preference ($SP = \delta^{15}N^{\alpha} - \delta^{15}N^{\beta}$), and $\delta^{18}O$ of N_2O ($\delta^{18}O$-N_2O), we estimate that nitrifier-denitrification produced between 11% and 26% of N_2O from cultures grown under 20% O_2 and 43% to 87% under 0.5% O_2. We also demonstrate that a positive correlation between SP and $\delta^{18}O$-N_2O is expected when nitrifying bacteria produce N_2O. A positive relationship between SP and $\delta^{18}O$-N_2O has been observed in environmental N_2O datasets, but until now, explanations for the observation invoked only denitrification. Such interpretations may overestimate the role of heterotrophic denitrification and underestimate the role of ammonia oxidation in environmental N_2O production.

Correspondence to: C. H. Frame
(cframe@whoi.edu)

1 Introduction

The atmospheric concentration of the greenhouse gas nitrous oxide (N_2O) has risen steadily over the last century. Processes in the microbial nitrogen cycle are the largest source of atmospheric N_2O and 20% of this source may come from the oceans (IPCC, 2007). Humans have greatly increased the amount of fixed nitrogen entering the oceans (Galloway et al., 1995), and the functioning of marine microbial ecosystems is shifting in response (Fulweiler et al., 2007; Beman et al., 2005; Naqvi et al., 2000). Understanding the impact of anthropogenic activity on the size of the marine N_2O source requires knowledge of which microbes are involved in N_2O production and how the production is controlled by chemical variables.

Published by Copernicus Publications on behalf of the European Geosciences Union.

Nitrification, and in particular ammonia oxidation, is thought to dominate N_2O production in oxic water columns (Elkins et al., 1978; Cohen and Gordon, 1979; Goreau et al., 1980; Ostrom et al., 2000; Popp et al., 2002). Oversaturations of dissolved N_2O (ΔN_2O, nmol L^{-1}) are often positively correlated with apparent oxygen utilization (AOU, µmol L^{-1}) (Yoshinari, 1976; Cohen and Gordon, 1978; Elkins et al., 1978). AOU is a tracer of organic matter remineralization. Therefore, the direct relationship between AOU and ΔN_2O is taken as evidence that N_2O is produced as nitrifying organisms convert regenerated NH_3 to NO_2^- and NO_3^-.

Stoichiometric relationships among N_2O production, NO_3^- regeneration, and AOU have been used to convert oceanographic nutrient and O_2 data to estimates of N_2O production (e.g., Codispoti and Christensen, 1985; Fuhrman and Capone, 1991; Jin and Gruber, 2003; Suntharalingam and Sarmiento, 2000) or to use N_2O concentration data to calculate nitrification rates (e.g., Law and Ling, 2001). However, there is not a universal AOU:N_2O ratio and linear AOU:N_2O relationships break down unpredictably in low-O_2 environments (Cohen and Gordon, 1979). Several different factors may contribute to this break-down: 1) at low O_2 concentrations, ammonia-oxidizing bacteria produce higher yields of N_2O per mole of NH_3 oxidized (Goreau et al., 1980; Lipschultz et al., 1981; Jorgensen et al., 1984), 2) heterotrophic denitrifying bacteria produce more N_2O in low-O_2 conditions (Knowles et al., 1981; Payne et al., 1971), 3) in stably anoxic environments denitrifying bacteria are net consumers of N_2O, which they reduce to nitrogen gas (N_2) (Cline et al., 1987), and 4) mixing between waters with different chemical properties influences the slopes of AOU:N_2O linear regressions (Nevison et al., 2003). There is also potential niche overlap among nitrifiers and denitrifiers in low-O_2 environments, making it especially difficult to distinguish between these two N_2O sources. Ammonia-oxidizing bacteria are able to thrive at low O_2 concentrations (Carlucci and McNally, 1969; Goreau et al., 1980; Codispoti and Christensen, 1985) and it has been suggested that denitrification occurs in oxic ocean waters in the anaerobic interiors of organic particles (Yoshida et al., 1989; Alldredge and Cohen, 1987). To understand how the N_2O budget may respond to global change, we need methods for determining the individual contributions of nitrification and denitrification to the N_2O budget.

Understanding the N_2O source from ammonia-oxidizing bacteria is particularly complicated because these organisms contain two distinct N_2O-producing pathways that may respond differently to geochemical controls. One pathway is the oxidative decomposition of hydroxylamine (NH_2OH), or one of its derivatives, during the conversion of NH_3 to NO_2^- (Hooper and Terry, 1979). The other mechanism, known as nitrifier-denitrification, is the sequential reduction of NO_2^- to NO and then N_2O by the action of the nitrite reductase (NIR, encoded by the gene *nirK*) and the nitric oxide reductase (NOR, encoded by the gene *norB*). All of the ammonia-oxidizing bacteria that have been screened to date contain the *nirK* and *norB* genes (Casciotti and Ward, 2001; Shaw et al., 2006; Casciotti and Ward, 2005; Cantera and Stein, 2007; Norton et al., 2008; Arp et al., 2007), and the conversion of $^{15}NO_2^-$ to $^{15}N_2O$ has been demonstrated in several genera (Poth and Focht, 1985; Shaw et al., 2006). Archaeal ammonia oxidizers also appear to possess *nirK* and *norB* homologs (Treusch et al., 2005; Hallam et al., 2006; Walker et al., 2010) but it is not known whether the proteins encoded by these genes are involved in N_2O production.

The enzymes involved in nitrifier-denitrification are homologous to those found in a subset of heterotrophic denitrifying bacteria. However, unlike heterotrophic denitrification, nitrifier-denitrification may not be a strictly anaerobic process (Shaw et al., 2006). Ammonia-oxidizing bacteria express *nirK* in aerobic environments in response to NO_2^- (Beaumont et al., 2004) and it has been hypothesized that NIR's main role is in detoxifying NO_2^- (Poth and Focht, 1985; Beaumont et al., 2002). Nevertheless, a role for O_2 is suggested by the fact that *nirK* expression increases in low-O_2 conditions (Beaumont et al., 2004), and yields of N_2O from cultures of ammonia-oxidizing bacteria increase more than 40-fold when O_2 concentrations drop below 5 µM (Goreau et al., 1980).

N_2O with biologically distinct origins can be identified using stable isotopic signatures. The oxygen isotopic signature (δ^{18}O-N_2O) has been used to distinguish nitrification and denitrification N_2O sources (Ostrom et al., 2000; Toyoda et al., 2005; Wrage et al., 2005; Kool et al., 2007). The δ^{18}O of N_2O depends on the proportion of oxygen in N_2O that is derived from O_2 vs. H_2O, as well as any fractionation factors associated with incorporation or loss of the oxygen atoms in the metabolic precursors of N_2O (Fig. 1) (Casciotti et al., 2010). N_2O derived from NH_2OH contains only oxygen atoms from O_2 whereas N_2O produced by nitrifier-denitrification or heterotrophic denitrification depends on the δ^{18}O of NO_2^- (and the δ^{18}O of NO_3^-, in the case of heterotrophic denitrification), which is derived from both O_2 and H_2O (Andersson et al., 1982; Casciotti et al., 2010; Buchwald and Casciotti, 2010). Since the δ^{18}O values of marine H_2O are typically at least 20‰ less than those of dissolved O_2 (Kroopnick and Craig, 1976), marine N_2O produced with different amounts of oxygen from H_2O and O_2 will reflect this in the δ^{18}O signature. Indeed, positive correlations between oceanographic δ^{18}O-O_2 and δ^{18}O-N_2O data have been interpreted as evidence that the N_2O is a product of nitrification because oxygen from O_2 is most directly incorporated into N_2O through NH_2OH during NH_3 oxidation (Ostrom et al., 2000; Andersson and Hooper, 1983).

However, there may be isotope effects associated with the incorporation of oxygen atoms from O_2 and H_2O into N_2O (Casciotti et al., 2010). If these isotope effects are significant and variable among different species of ammonia oxidizers, it may prove difficult to extract source information

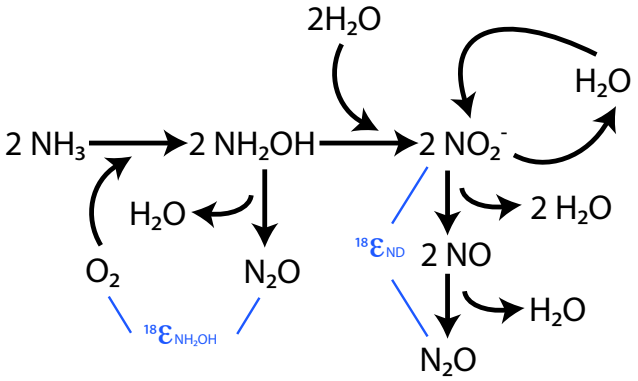

Fig. 1. During ammonia oxidation, the oxygen atoms incorporated into N_2O come from either O_2 or H_2O. The δ^{18}O-N_2O depends upon the isotopic signatures of these two substrates as well as isotope effects ($^{18}\epsilon$) that may be associated with the individual formation mechanisms, hydroxylamine ($^{18}\epsilon_{NH2OH}$) decomposition and nitrifier-denitrification of nitrite ($^{18}\epsilon_{ND}$).

based on oxygen isotopes alone. Furthermore, the δ^{18}O of N_2O produced by ammonia-oxidizing bacteria may change depending on what fraction of the oxygen atoms are derived from O_2 (via NH_2OH decomposition and nitrifier-denitrification) vs. H_2O (via nitrifier-denitrification) (Fig. 1).

The ^{15}N site preference (SP) is another isotopic signature used to interpret environmental N_2O data (Toyoda et al., 2002; Sutka et al., 2003, 2004; Toyoda et al., 2005; Sutka et al., 2006; Koba et al., 2009). SP as defined by Toyoda and Yoshida (1999) is the difference in the isotopic enrichment of the internal (α) and external (β) nitrogen atoms in the linear N_2O molecule:

$$SP = \delta^{15}N^{\alpha} - \delta^{15}N^{\beta}.$$

Unlike δ^{18}O and $\delta^{15}N^{bulk}$ values, SP is thought to reflect the N_2O production mechanism while remaining independent of the substrate's isotopic signature. This is because the reactions that produce N_2O involve two identical precursor molecules (either NO or NH_2OH) (Toyoda et al., 2002; Schmidt et al., 2004) that are presumably drawn simultaneously from the same substrate pool. SP measurements made on N_2O produced by ammonia-oxidizing bacteria and denitrifying bacteria support this idea (Sutka et al., 2006). Cultures of ammonia-oxidizing bacteria produce N_2O with a SP of about 33.5‰ via NH_2OH decomposition. However, in the presence of NO_2^- and low O_2 concentrations, the same bacteria make N_2O with a SP that is closer to that of denitrifying bacteria (−0.8‰) (Sutka et al., 2003, 2004, 2006).

Previous workers have estimated the "end-member" SP signatures for the two different sources of N_2O in ammonia oxidizer cultures by manipulating O_2 concentrations in order to favor production via one process over the other (Sutka et al., 2003, 2004, 2006). However, since NH_2OH decomposition and nitrifier-denitrification can give rise to N_2O simultaneously, failure to account for this mixing may cause errors in these end-member SP estimates. If N_2O from NH_2OH decomposition has a SP that is much higher than the SP of N_2O from nitrifier-denitrification, as proposed by Sutka et al. (2003, 2004, 2006), then source mixing would cause underestimation of the SP of NH_2OH decomposition and overestimation of the SP of nitrifier-denitrification.

Here we have used δ^{18}O-N_2O and SP measurements to make mixing-corrected estimates of the end-member SP values for N_2O produced by NH_2OH decomposition and nitrifier-denitrification by the marine ammonia-oxidizing bacterium *Nitrosomonas marina* C-113a. These end-member values were then used to calculate the N_2O yields from nitrification and nitrifier-denitrification in different growth conditions, including a range of O_2 headspace concentrations (20%, 2%, and 0.5%), excess NO_2^- (0.2 to 1 mM), at different cell densities, and in the presence of nitrite-oxidizing bacteria. Each experiment was carried out with an eye towards simulating environmental conditions more closely than previous studies by using growth medium that contains a fraction of the NH_4^+ present in commonly used recipes for ammonia oxidizer media (50 µM vs. 5 to 10 mM NH_4^+), and lower cell densities.

2 Materials and methods

2.1 Culture maintenance and experimental setup

Nitrosomonas marina C-113a cultures were maintained semi-continuously in Watson medium containing 5 mM NH_4^+ (Watson, 1965). All maintenance cultures were kept in the dark at 22 °C with shaking at 100 rpm. The cultures used to inoculate experiments were periodically tested for heterotrophic contamination as follows: 1 ml of each culture was added to 2 ml of a sterile 1:4 mixture of tryptic soy broth and artificial seawater and incubated 3 to 4 weeks in aerated culture tubes. Contamination was of particular concern during experiments on high density C-113a cultures because the abundance of cellular material was a potential source of organic substrate for the growth of heterotrophic denitrifiers, which can also produce N_2O at low O_2 concentrations. For this reason, additional purity tests were done by inoculating 5 ml of each high density culture ($10^5 - 10^6$cells ml^{-1}) into 10 ml of the sterile tryptic soy/artificial seawater mixture amended with 1 mM $NaNO_2$. These cultures were incubated in closed, inverted 15 ml centrifuge tubes for 3 to 4 weeks. All tubes remained free of turbidity and showed no production of gas bubbles that would indicate heterotrophic denitrification.

Experiments were carried out in 545 ml glass serum bottles (Wheaton, 223952) that contained 100 ml sterile Watson medium with 50 µM NH_4^+. Parallel experiments in ^{18}O-enriched water were set up by adding 1 ml of 5000‰ δ^{18}O-H_2O into each bottle. The headspace of each bottle

was sealed using 30 mm gray butyl rubber septa (Wheaton, 224100-331) and aluminum crimps (Wheaton, 224187-01). Atmospheric O_2 and N_2O were removed by purging for 3 h with N_2 flowing at > 60 ml min^{-1} and appropriate amounts of high-purity O_2 ($\delta^{18}O = +25.3‰$) were injected back into each headspace to achieve 20%, 2%, or 0.5% O_2 (v/v) (203, 20, or 5 µM dissolved O_2, respectively). Headspace O_2 and N_2O concentrations were checked before and after each experiment by electron capture gas chromatography (see below). The ratio of headspace to liquid volumes was such that complete NH_3 oxidation consumed less than 10% of the total O_2 in the lowest O_2 headspaces.

Immediately before each experiment, 1–2 l of late exponential or early stationary phase cultures were centrifuged at 10 000 g for 30 min, washed to remove residual NH_4^+ and NO_2^-, and re-suspended in 30 ml sterile media without NH_4^+. Experiments were initiated by the injection of 500 µl of washed and resuspended cells into each bottle. In the co-culture experiments, ammonia oxidizers with cell densities of approximately 2×10^5 cells ml^{-1} were added with washed and resuspended cells of the nitrite oxidizer *Nitrococcus mobilis* (10^6 cells ml^{-1}).

Initial and final cell densities were measured in samples preserved with 2% formalin (0.22-µm filtered) by making microscopic counts of DAPI-stained cells, or by using fluorescence assisted flow cytometry (FACS) to count SYBR green-stained cells on a FACS Calibur flow cytometer (Becton Dickinson). Uninoculated bottles served as a control for abiotic N_2O production and were analyzed in parallel with experimental bottles. All bottles were incubated in the dark at room temperature with constant shaking. The progress of NH_3 oxidation was monitored by measuring accumulation of NO_2^- and disappearance of NH_4^+ from the medium (see below). Once NH_3 oxidation was complete, experiments were terminated by injecting each bottle with 1 ml of 6 M NaOH, lysing the cells.

2.2 Chemical analyses

The concentrations of NH_4^+ were determined colorimetrically by the phenol-hypochlorite method (Solorzano, 1969) and NO_2^- concentrations were determined by the Griess-Ilosvay colorimetric method (Pai and Yang, 1990) using a 1 cm path-length flow cell. Headspace O_2 concentrations were determined using a gas chromatograph with a ^{63}Ni electron capture detector (Shimadzu GC-8A). The O_2 peaks from 20 to 250 µl injections of sample headspace were recorded and integrated using Shimadzu EZStart software (v. 7.2.1). Sample peak areas were calibrated with standard injections of air. Headspace N_2O concentrations were also measured before and after each experiment using the GC-8A. Sample peak areas were calibrated against commercial N_2O mixtures (10, 1, and 0.1 ppm) and fresh atmospheric air (approximately 320 ppb). When total headspace N_2O was less than 20 nmol, N_2O was quantified by analyzing the whole bottle (by purging and trapping, see below) on a Finnigan Delta^{PLUS} Isotope ratio mass spectrometer (IRMS) and using the linear relationship between peak area of *m/z* 44 and nanomoles of N_2O to determine total N_2O. The average blank determined by analyzing bottles flushed with high-purity N_2 was 0.08 ± 0.04 nmol N_2O.

2.3 Isotopic analyses

Isotopic analyses of N_2O were conducted using a Finnigan Delta^{PLUS} XP IRMS. Bottles were purged with He and N_2O was cryo-trapped on-line with a custom-built purge and trap system (McIlvin and Casciotti, 2010) operated manually with 545 ml serum bottles. The following modifications made large volume gas extraction possible: bottles were loaded manually, the helium flow rate was increased to 60 ml min^{-1}, and the purge time was extended to 45 min. As described in McIlvin and Casciotti (2010), CO_2 was largely removed from the gas stream by passage through a Carbosorb trap, then N_2O was separated from residual CO_2 using a capillary column (25 m × 0.32 mm) lined with Poraplot-Q before injection into the mass spectrometer through an open split. Mass/charge *(m/z)* peak areas were automatically integrated using Isodat 2.0 software. Values for $\delta^{18}O$-N_2O, $\delta^{15}N^{bulk}$, $\delta^{15}N^{\alpha}$, and $\delta^{15}N^{\beta}$ were obtained from the 45/44, 46/44, and 31/30 peak area ratios and referenced to our laboratory's N_2O tank as described in Appendix A. This reference tank has been calibrated for $\delta^{18}O$-N_2O (‰ vs. VSMOW), $\delta^{15}N^{bulk}$, $\delta^{15}N^{\alpha}$, and $\delta^{15}N^{\beta}$ (‰ vs. AIR) by S. Toyoda (Tokyo Institute of Technology). Furthermore, the isotopomer-specific NO^+ fragment ion yields for our Delta^{PLUS} XP were determined for the ion source conditions used in these measurements (see Appendix B). For quality-control, two or three tropospheric N_2O samples were analyzed between every 7 to 10 experimental samples to check the consistency of our isotopomer analyses. These samples were created by allowing 100 ml of artificial seawater to equilibrate with outside air in 545 mL serum bottles, sealing the bottles, and analyzing them as described above. Triplicate samples of tropospheric N_2O from Woods Hole, MA analyzed during a typical run had $\delta^{15}N^{\alpha} = 15.0 \pm 0.1‰$, $\delta^{15}N^{\beta} = -1.9 \pm 0.1‰$, $\delta^{18}O = 44.4 \pm 0.2‰$, $\delta^{15}N^{bulk} = 6.5 \pm 0.1‰$, SP = $16.9 \pm 0.1‰$, and *m/z* 44 peak area = 15.6 ± 0.2 mV-s (7.8 ± 0.1 nmol).

We also measured the $\delta^{18}O$ and $\delta^{15}N$ of NO_2^- that was produced by cultures as NH_3 oxidation progressed. NO_2^- was converted to N_2O using the azide method developed by McIlvin and Altabet (2005). The conversion to N_2O was carried out immediately after sampling to avoid shifts in the oxygen isotopic values by abiotic exchange with water (Casciotti et al., 2007) or continued biological production of NO_2^- from residual NH_3. Individual sample volumes were adjusted so that a consistent amount of N_2O (5 or 10 nmol) was produced for each set of azide reactions. Each sample set included at least three sets of three different NO_2^- standards (N-23,

N-7373, and N-10219; Casciotti et al., 2007) that were used to calculate sample δ^{15}-NO_2^- (‰ vs. AIR) and δ^{18}O-NO_2^- (‰ vs. VSMOW) values. These samples were analyzed in 20 ml headspace vials using the autosampler setup described by Casciotti et al. (2002), modified with the addition of an −60 °C ethanol trap and column backflush (McIlvin and Casciotti, 2010).

3 Results and discussion

Nitrifier-denitrification depends on the presence of NO_2^- to produce N_2O (Ritchie and Nicholas, 1972; Poth and Focht, 1985; Yoshida, 1988), and the accumulation of NO_2^- in environments such as oxygen deficient zones (ODZs) could contribute to increased N_2O production in these regions. To date, the roles of substrate concentration and cell density in determining N_2O yield have not been systematically investigated. This study was designed to test the impact of O_2 and NO_2^- concentrations on the N_2O yield of marine ammonia-oxidizing bacteria at a lower substrate (NH_3) concentration, and at a broader and lower range of cell densities than any previous work. N_2O yield data are presented in the same form used in oceanographic N_2O studies so that yields are the fraction of N-atoms converted to N_2O out of the total amount of NH_3 that is oxidized (i.e. 2 × moles N_2O/moles NH_3). In other words, a yield of 5×10^{-4} indicates that 1 in every 2000 N-atoms from oxidized NH_3 will go into an N_2O molecule.

3.1 Cell density and O_2 concentration

Cell density influenced the observed N_2O yields in both low O_2 (0.5% and 2%) and high O_2 (20%) conditions. O_2 concentration had the greatest impact on N_2O yield at the highest starting cell density tested (1.5×10^6 cells ml^{-1}) (Fig. 2). At 20% O_2, the high density cultures had the lowest average yields observed, ($1.3 \pm 0.4 \times 10^{-4}$) while at 0.5% O_2 the high density cultures had the highest average yields observed ($220 \pm 40 \times 10^{-4}$). In contrast, O_2 had a much smaller impact on N_2O yield in the medium density cultures (starting density = 2.1×10^4 cells ml^{-1}) and the low density cultures (starting density = 2×10^2 cells ml^{-1}). In fact, the N_2O yields of the medium density cultures were not significantly different among the high and low O_2 treatments (at 20% O_2, $5.1 \pm 0.5 \times 10^{-4}$, at 2% O_2, $5.5 \pm 0.8 \times 10^{-4}$, and at 0.5% O_2, $6.4 \pm 1.4 \times 10^{-4}$). Low density cultures produced average yields of $3.9 \pm 0.3 \times 10^{-4}$ at 20% O_2, $4.7 \pm 0.1 \times 10^{-4}$ at 2% O_2, and $6.7 \pm 0.5 \times 10^{-4}$ at 0.5% O_2.

The average yields of the cultures at 20% O_2 were comparable to the production yields ($0.8 - 5.4 \times 10^{-4}$) measured by Yoshida et al. (1989) in the oxic surface waters of the western North Pacific using $^{15}NH_4^+$ tracer techniques. However, they are lower than previously reported yields for *Nitrosomonas* cultures at 20% O_2 ($26 - 30 \times 10^{-4}$ in Goreau et al. (1980) and $10 - 390 \times 10^{-4}$ in Remde and Conrad, 1990).

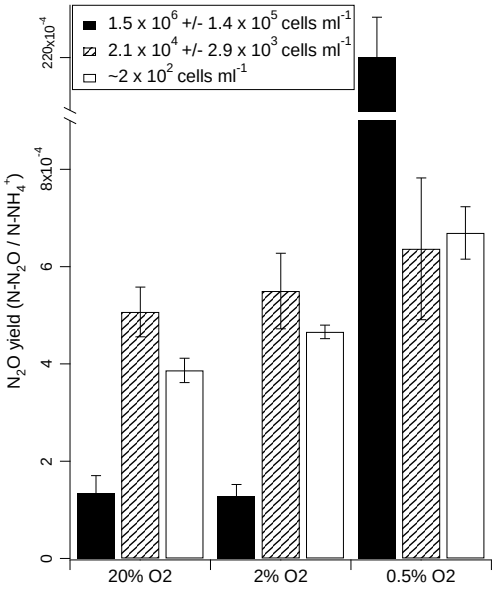

Fig. 2. N_2O yields vs. cell density. Each bar represents the average of 5 replicate cultures. Error bars are for one standard deviation among replicates.

In this study, low-O_2 conditions only resulted in substantial increases in N_2O yield when cell densities were greater than 10^6 cells ml^{-1}. N_2O yields were relatively low and less sensitive to O_2 when cell densities were closer to those observed in the ocean (10^3–10^4 cells l^{-1}; Ward et al., 1982). This draws into question the oceanographic applicability of previous culture-based yield measurements, where a many-fold increase in N_2O yield was observed as O_2 dropped from 20% to 0.5% (Goreau et al., 1980). Goreau et al. (1980) worked with a marine *Nitrosomonas* strain at cell densities (1×10^6 cells ml^{-1}) comparable to our high density experiments and observed N_2O yields of $800 - 1000 \times 10^{-4}$ for cultures grown at 0.5% O_2 on 24 mM NH_4^+. The implication of the present study is that factors such as cell density can influence the relationship between N_2O yield and O_2 concentration.

The mechanisms that explain the high N_2O yields of high density cultures at low O_2 could be chemical or biological. O_2 has a major influence on the half-life of nitric oxide (NO), the gaseous precursor of N_2O during nitrifier-denitrification. Therefore, concentration-dependent changes in the rate of N_2O-production could be related to O_2 as a consequence of the abiotic oxidation of NO:

$$2NO + O_2 \rightarrow 2NO_2$$

$$2NO_2 + H_2O \rightarrow HNO_2 + HNO_3, \text{ (Ritchie and Nicholas, 1972),}$$

where nitrous acid (HNO_2), is the major decomposition product of the second reaction (Ignarro et al., 1993). In aerobic environments, O_2 is the major reactant and any NO present reacts away soon after it is produced (Lewis and

Deen, 1994). However, in low-O_2 environments the half-life of NO increases, so that during bacterial NH_3 oxidation, it can accumulate to concentrations that are similar to N_2O (Remde and Conrad, 1990; Lipschultz et al., 1981). This may allow the enzymes that carry out NO reduction to compete for NO with the above O_2-dependent reaction. Studies of *N. europaea* have also shown that the expression of *nirK* during nitrifier-denitrification is controlled by a repressor protein (Beaumont et al., 2002, 2004) that belongs to a family of NO-sensitive transcription regulators (Rodionov et al., 2005). If NO induces *nirK* transcription, the abiotic reaction of O_2 with NO could reduce NIR-dependent N_2O production by consuming the inducer. Finally, high cell densities may be necessary for either of these effects to become important because the ability of NO-reducing enzymes to compete with O_2 for NO will depend on the diffusivities of O_2 and NO relative to the average distance between cells.

It is unclear why cultures with the highest cell densities had significantly lower N_2O yields at 20% O_2 than cultures with lower densities (Fig. 2). Time, NO_2^- (or NO), and increasing cell numbers could all enhance N_2O production by nitrifier-denitrification. There were significant differences in the amount of time that it took cultures of each density to oxidize all the NH_4^+ present. The low and medium density cultures took 14 and 3.5 d to oxidize 50 µM NH_4^+, respectively, while the high density cultures took only 7 h. Cell numbers also doubled approximately 7, 2, and 0 times, in the low, medium, and high density cultures, respectively. Thus, in the low and medium density cultures, NO_2^- and cells accumulated over longer periods of time than they did in the high density cultures. Further research is needed to determine the behavioral and/or kinetic effects that influence the N_2O yields from ammonia oxidizers.

3.2 NO_2^- and O_2 concentration

In pure batch cultures of ammonia oxidizers, NO_2^- exposure is an unavoidable result of growth because NO_2^- accumulates up to the initial NH_4^+ concentration. Excess NO_2^- may increase N_2O yields if ammonia oxidizers convert NO_2^- to N_2O to avoid the toxic effects of NO_2^- (Poth and Focht, 1985; Beaumont et al., 2002, 2004). To test the impact of NO_2^- on N_2O yields, we increased NO_2^- concentrations by adding 0.2 or 1 mM NO_2^- to some cultures, and decreased accumulated NO_2^- concentrations in others by adding the nitrite-oxidizing bacterium *Nitrococcus mobilis* to create a co-culture.

In the co-cultures, NO_2^- concentrations remained below detection at 20% O_2 and below 17 µM at 0.5% O_2. Although co-culturing kept NO_2^- concentrations lower than they were in the pure cultures, N_2O yields were not significantly lower in the presence of the nitrite-oxidizing bacteria (Fig. 3a). The insignificant differences between the yields with and without nitrite oxidizers suggests that the 50 µM NO_2^- that accumulated in our pure cultures did not have a major impact on the N_2O yields measured for those cultures. However, we were unable to entirely eliminate NO_2^- accumulation in the low-O_2 experiments. Future work should focus on identifying the impact of NO_2^- on N_2O production by nitrifiers in low-O_2 environments.

The addition of 1 mM NO_2^- had a greater impact on N_2O yield than the differences in O_2 concentration did (Fig. 3b). The increase due to the additional NO_2^- was apparent in both low and high O_2 conditions. Furthermore, the average N_2O yields increased as the amount of added NO_2^- increased. Cultures under 20% O_2 with no added NO_2^- had an average yield of $4.0 \pm 0.03 \times 10^{-4}$ while those with 1 mM added NO_2^- had an average yield of $7.6 \pm 0.5 \times 10^{-4}$. Cultures under 0.5% O_2 with no added NO_2^- had an average yield of $6.0 \pm 0.5 \times 10^{-4}$ and those with 1 mM added NO_2^- had an average yield of $10.2 \pm 0.3 \times 10^{-4}$. N_2O yields were calculated as a fraction of the total N in NH_4^+ consumed during the experiment ($\simeq 5 \times 10^{-6}$ moles).

From this work, it is clear that increased NO_2^- concentrations enhance N_2O production in cultures of ammonia-oxidizing bacteria. This is consistent with a detoxification role for nitrite reductase in nitrifying bacteria, as suggested by previous work (Beaumont et al., 2004). The relationship between NO_2^-, nitrifier-denitrification, and N_2O production is also complex. Aerobic *nirK* expression occurs in response to increasing NO_2^- concentrations (Beaumont et al., 2004), but *nirK* knock-out mutants actually produce more N_2O than the wild-type strain. The authors suggest that the NH_2OH-dependent pathway has a role in this increase (Beaumont et al., 2002).

Oceanic O_2 concentrations may influence a number of different biogeochemical variables that enhance N_2O production by ammonia oxidizers. For example, low dissolved O_2 concentrations are often associated with elevated NO_2^- concentrations (Codispoti et al., 2001). When dissolved O_2 concentrations are low, the biological turnover time of NO_2^- also increases (Hashimoto et al., 1983) in part because the activity of nitrite-oxidizing bacteria ceases at a higher O_2 concentration than the activity of ammonia-oxidizing bacteria (Helder and de Vries, 1983). Charpentier et al. (2007) also suggest that high concentrations of organic particles found in certain productive waters enhance N_2O production by creating high-NO_2^-, low-O_2 microenvironments necessary to support nitrifier-denitrification. Future oceanographic work should investigate how N_2O production rates in oxygen deficient zones (ODZs) relate to these different biogeochemical variables.

3.3 Pathway dependence of $\delta^{15}N^{bulk}$-N_2O

Ammonia-oxidizing bacteria make N_2O through two different pathways, so that the observed isotopic signatures of N_2O are a function of the pathways' mixing fractions, the isotopic signatures of their different substrate molecules,

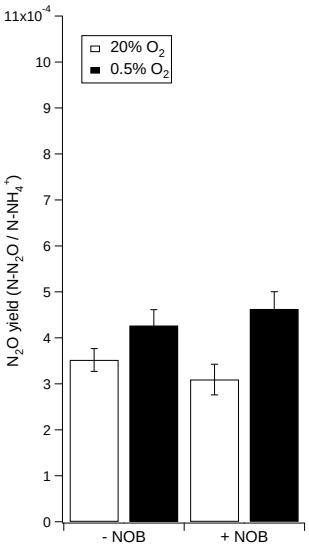

Fig. 3a. N_2O yields in the presence and absence of nitrite-oxidizing bacteria (NOB). Starting NH_4^+ concentrations were 50 µM.

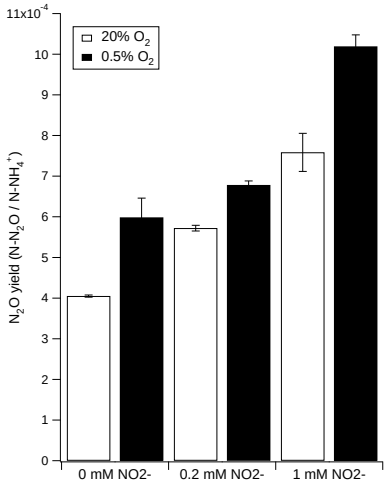

Fig. 3b. N_2O yields increased when NO_2^- was added to the starting media. Initial NH_4^+ concentrations were 50 µM. Added NO_2^- was either 0, 0.2 mM, or 1 mM.

and the different isotope effects associated with those pathways. Complete biochemical decoupling of the nitrifier-denitrification pathway from the NH_2OH decomposition pathway is difficult to achieve with intact C-113a cells because the bacteria require NH_3 to support their respiratory electron transport chain, and N_2O production stops once NH_3 oxidation is complete (Supplementary Fig. S.3). Therefore, while we manipulated growth conditions such as O_2 concentration and cell density in order to favor one N_2O production mechanism over another, in interpreting the results we account for N_2O contributions from both sources.

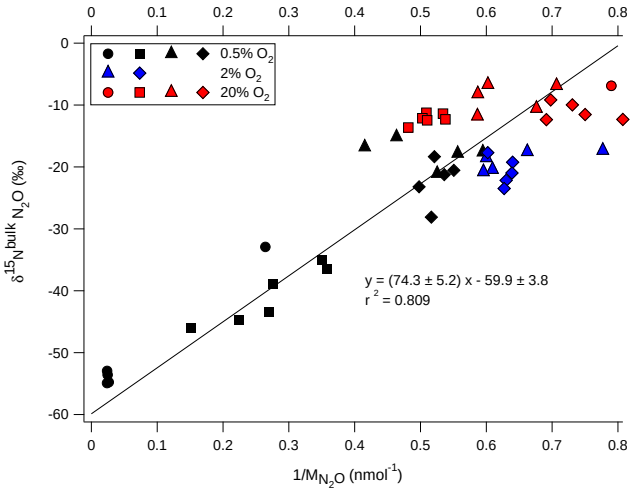

Fig. 4. Pathway dependence of $\delta^{15}N^{bulk}$ N_2O. Symbol shapes correspond to different starting cell densities: circles correspond to 1.5×10^6 cells ml^{-1}, squares to 2×10^5 cells ml^{-1}, triangles to 2.1×10^4 cells ml^{-1}, and diamonds to 2×10^2 cells ml^{-1}. Colors correspond to headspace O_2 levels, with black symbols representing 0.5% O_2, blue symbols 2% O_2, and red symbols 20% O_2. The slope and intercept of a Type II linear regression of $\delta^{15}N^{bulk}$ and $1/M_{N_2O}$ are given ± one standard deviation. In making a linear fit to the data, we assume that any differences in total N_2O are due to nitrifier-denitrification. The y-intercept of the line is equal to the $\delta^{15}N^{bulk}$ of N_2O from nitrifier-denitrification. Data points that were less than 1 nmol N_2O were not included.

N_2O produced by all C-113a cultures was depleted in ^{15}N relative to the substrate ($\delta^{15}N$-$NH_4^+ = -3$‰), although the range varied widely ($\delta^{15}N^{bulk}$-$N_2O = -54.9$‰ to -6.6‰, Fig. 4). Culture conditions affected the degree of ^{15}N depletion, with cultures grown under 0.5% O_2 producing the most depleted N_2O (-54.9‰ to -15.2‰), while cultures grown with 20% O_2 generally produced N_2O with higher $\delta^{15}N$ values (-13.6‰ to -6.7‰). The low-O_2 cultures that produced the most depleted N_2O also produced the most N_2O (the highest yield). We interpret the observed variation in $\delta^{15}N^{bulk}$-N_2O to have arisen from pathway-dependent mixing, which implies that a single isotope effect will not adequately relate the $\delta^{15}N^{bulk}$-N_2O to the substrate nitrogen compounds.

We assume that each datapoint ($\delta^{15}N^{bulk}_{total}$, M_{total}, where M refers to moles of N_2O) represents a two-component mixture of a constant or "basal" N_2O source from NH_2OH decomposition (M_{NH_2OH}) and a variable source of N_2O from nitrifier-denitrification (M_{ND}) that tended to be larger in low-O_2 cultures. This is the basis for performing the type II linear regression of $\delta^{15}N^{bulk}$ vs. $\frac{1}{M_{N_2O}}$ in Fig. 4. Equation (3b), the model for the linear regression was developed using the mass balance Eqs. (1 and 2) (Table 1).

According to Eq. (3b), the y-intercept of the regression is the $\delta^{15}N^{bulk}$ of the more depleted nitrifier-denitrification

Table 1. Equations used to model the $\delta^{15}N^{bulk}N_2O$ data in Fig. 4.

(1) $\delta^{15}N^{bulk}_{total} \times M_{total} = \delta^{15}N^{bulk}_{ND} \times M_{ND} + \delta^{15}N^{bulk}_{NH_2OH} \times M_{NH_2OH}$
(2) $M_{ND} = M_{total} - M_{NH_2OH}$
(3a) $\delta^{15}N^{bulk}_{total} = \frac{\delta^{15}N^{bulk}_{ND} \times (M_{total} - M_{NH_2OH}) + \delta^{15}N^{bulk}_{NH_2OH} \times M_{NH_2OH}}{M_{total}}$
(3b) $\delta^{15}N^{bulk}_{total} = (\delta^{15}N^{bulk}_{NH_2OH} \times M_{NH_2OH} - \delta^{15}N^{bulk}_{ND} \times M_{NH_2OH}) \times \frac{1}{M_{total}} + \delta^{15}N^{bulk}_{ND}$

end-member ($\delta^{15}N^{bulk}_{ND}$). This is because as the amount of N_2O approaches infinity, the $\delta^{15}N^{bulk}_{ND}$ should overwhelm the basal end-member signature, $\delta^{15}N^{bulk}_{NH_2OH}$.

The value of $\delta^{15}N^{bulk}_{ND}$ obtained in this way is -59.9‰, ± 3.8‰ (errors are given as one standard deviation of the y-intercept). The difference between the $\delta^{15}N^{bulk}$ of the product N_2O and the $\delta^{15}N$ of the substrate NH_3 is the overall isotope effect associated with N_2O formation by nitrifier-denitrification ($^{15}\epsilon_{ND} = -56.9$‰). The most enriched N_2O produced in these experiments had a $\delta^{15}N^{bulk}$ of -6.7‰, providing a minimum for $\delta^{15}N^{bulk}_{NH_2OH}$. This is a minimum because if a fraction of this N_2O was produced by nitrifier-denitrification, we would not observe the heaviest possible value for the NH_2OH end-member.

This end-member mixing model does not account for the Rayleigh effects that kinetic isotopic fractionation has in closed systems such as batch cultures. These effects change the isotopic signatures of the NH_3 that is consumed and the NO_2^- that accumulates as NH_3 oxidation proceeds (Mariotti et al., 1981) so that at any instant during the reaction, the $\delta^{15}N$ of N_2O produced from these substrates will also reflect these isotopic shifts. However in this study, the end-member mixing model is not a serious violation of Rayleigh assumptions because all cultures were allowed to oxidize the same amount of NH_3 to completion before the total N_2O was analyzed. Abrupt changes in N_2O production rates during the NH_3 oxidation reaction could also make this model problematic in a Rayleigh system. In these experiments, however, N_2O accumulated steadily as NH_3 oxidation progressed and NO_2^- accumulated (Supplementary Fig. S.3).

3.4 Covariation of SP and $\delta^{18}O$-N_2O

The $\delta^{18}O$ of N_2O is like the $\delta^{15}N^{bulk}$ in that these signatures are both process-dependent and substrate-dependent. That is, the $\delta^{18}O$ of N_2O produced by ammonia-oxidizing bacteria depends on the mixing fraction of the two N_2O-producing pathways as well as the isotopic signatures of the substrates (O_2 and H_2O) that contribute oxygen atoms to those pathways and isotopic fractionation during oxygen atom incorporation or loss in the reactions that make N_2O (Fig. 1) (Casciotti et al., 2010). The conversion of NH_3 to NO_2^- incorporates oxygen atoms from O_2 in the first step and H_2O in the second step (Andersson et al., 1982; Andersson and Hooper, 1983):

$$NH_3 + \frac{1}{2}O_2 \rightarrow NH_2OH$$

$$NH_2OH + H_2O \rightarrow HNO_2 + 4H\cdot$$

We expect the $\delta^{18}O$ of N_2O derived from NH_2OH decomposition to be independent of the $\delta^{18}O$ of H_2O because O_2 is the sole contributor of oxygen during the first reaction. However, the $\delta^{18}O$ of N_2O produced by NO_2^- reduction during nitrifier-denitrification depends upon both the $\delta^{18}O$-O_2 and $\delta^{18}O$-H_2O, in proportions that are affected by the amount of oxygen atom exchange between NO_2^- and H_2O (Andersson and Hooper, 1983; Casciotti et al., 2002; Kool et al., 2007; Casciotti et al., 2010). The fact that the $\delta^{18}O$ of N_2O produced by nitrifier-denitrification is sensitive to changes in $\delta^{18}O$-H_2O is the basis for a technique that uses parallel experiments in ^{18}O-labeled and unlabeled H_2O to identify the proportion of N_2O produced by nitrifier-denitrification (Wrage et al., 2005).

The impact of the $\delta^{18}O$-H_2O on the $\delta^{18}O$ of N_2O produced by C-113a is demonstrated in Fig. 5, where cultures grown in water with a $\delta^{18}O$ of $+40$‰ (labeled) produced N_2O that was 5‰ to 40‰ more enriched in ^{18}O than cultures grown in H_2O with a $\delta^{18}O$ of -5‰ (unlabeled). The difference in $\delta^{18}O$-N_2O between labeled and unlabeled cultures was greatest at 0.5% O_2, when more N_2O was produced. At higher O_2 concentrations, less N_2O was produced and there was convergence of the $\delta^{18}O$-N_2O values from labeled and unlabeled experiments. The difference in $\delta^{18}O$-N_2O from ammonia oxidizers grown in labeled and unlabeled H_2O is directly proportional to the fraction of the total N_2O that is produced by nitrifier-denitrification. The pattern is consistent with relatively more N_2O production by nitrifier-denitrification as the O_2 concentration drops and H_2O contributes more to the overall $\delta^{18}O$-N_2O. Note that in these experiments, side-by-side comparisons between labeled and unlabeled replicates assume that nitrifier-denitrification and NH_2OH decomposition contribute the same proportion of N_2O to both labeled

Table 2. Equations used to model the SP and δ^{18}O-N_2O data in Figure 5.

(4a) $SP_{total} = F_{ND} \times SP_{ND} + (1 - F_{ND}) \times SP_{NH_2OH}$

(4b) $F_{ND} = \frac{SP_{total} - SP_{NH_2OH}}{SP_{ND} - SP_{NH_2OH}}$

(5) $\delta^{18}O\text{-}N_2O_{total} = F_{ND} \times (\delta^{18}O\text{-}NO_2^- - {}^{18}\epsilon_{ND}) + (1 - F_{ND}) \times (\delta^{18}O\text{-}O_2 - {}^{18}\epsilon_{NH_2OH})$

(6) $\delta^{18}O\text{-}N_2O_{total} = \frac{SP_{total} - SP_{NH_2OH}}{SP_{ND} - SP_{NH_2OH}} \times (\delta^{18}O\text{-}NO_2^- - \epsilon_{ND}) + (1 - \frac{SP_{total} - SP_{NH_2OH}}{SP_{ND} - SP_{NH2OH}}) \times (\delta^{18}O\text{-}O_2 - \epsilon_{NH_2OH})$

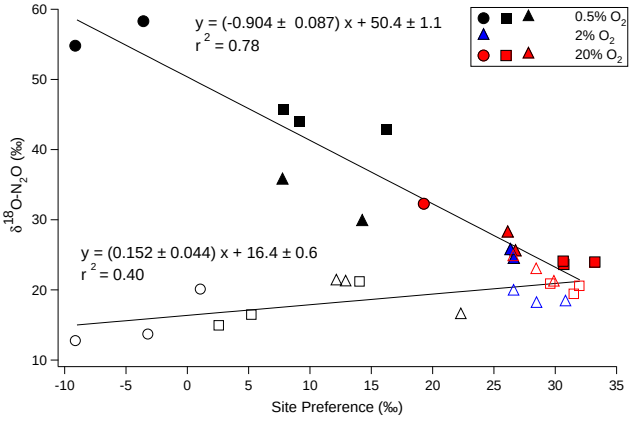

Fig. 5. Pathway dependence of δ^{18}O-N_2O and SP. Filled symbols are data from cultures grown in labeled water (about 40‰) while open symbols are data from cultures in unlabeled water (about −5‰). Circles correspond to cultures with cell densities of 1.5×10^6 cells ml^{-1}, squares to 2×10^5 cells ml^{-1}, and triangles to 2.1×10^4 cells ml^{-1}. Colors correspond to headspace O_2 levels, with black symbols representing 0.5% O_2, blue symbols 2% O_2, and red symbols 20% O_2. Regression slopes and intercepts are given ± one standard deviation. Data from low-density cultures were not included to avoid the impact of relaxation of the δ^{18}O-NO_2^- towards equilibrium with H_2O over the course of the NH_3 oxidation reaction. Data points that were less than 1 nmol N_2O were not included. All δ^{18}O values are referenced to VSMOW.

and unlabeled replicates and that the N_2O from NH_2OH decomposition has the same ^{18}O signature in both labeled and unlabeled experiments. This will be addressed in more detail below.

In contrast to δ^{18}O-N_2O, SP signatures of N_2O from ammonia oxidizers are thought to be process-dependent and substrate-independent: SP signatures vary as a result of mixing among N_2O sources with distinct SP values (Sutka et al., 2003, 2004, 2006), but they do not depend on the δ^{15}N values of the N_2O precursor molecules (Toyoda et al., 2002). In the present study, C-113a produced high-SP N_2O (up to 33.2‰) under 20% O_2 and low-SP N_2O (down to −9.1‰) under 0.5% O_2 (Fig. 5). Similar results have been observed for *N. europaea*, which produces high-SP N_2O (31.4 ± 4.2‰) when growing aerobically on NH_3, (Sutka et al., 2006) but can also produce low-SP N_2O (-0.8 ± 5.8‰) in the presence of NO_2^- and anaerobic conditions (Sutka et al., 2003, 2004).

Knowing the end-member SP signatures of N_2O from NH_2OH decomposition and nitrifier-denitrification is powerful because these values can then be used to calculate the size of each pathway's contribution to a culture's total N_2O output based on its SP signature (SP_{total}) (Charpentier et al., 2007). We developed the following model in order to extract these end-member SP signatures from our data while accounting for the fact that the SP of the N_2O from each culture is a mixture of these end-members. Following Charpentier et al. (2007), we set up a system of isotopic mass balance equations (Table 2) that describe isotopic mixing between low-SP N_2O from nitrifier-denitrification (SP_{ND}) and high-SP N_2O from NH_2OH decomposition (SP_{NH_2OH}), where F_{ND} is the fraction of total N_2O that is produced by nitrifier-denitrification. Solving Eq. (4a) for F_{ND} produces Eq. (4b) which cannot be solved for F_{ND} without knowing the end-member values, SP_{ND} and SP_{NH_2OH}, or having additional information about the value of F_{ND} for each data point. Therefore, we develop a complementary mixing equation based on the δ^{18}O-N_2O in Eq. (5) (Table 2).

As discussed above, the measured δ^{18}O-N_2O (δ^{18}O-N_2O_{total}) depends not only on the mixing fraction F_{ND}, but also the isotopic signatures of the substrate molecules (δ^{18}O-O_2 and δ^{18}O-NO_2^-) and kinetic and/or branching isotope effects associated with either reaction ($^{18}\epsilon_{NH_2OH}$ and $^{18}\epsilon_{ND}$). In these equations, $^{18}\epsilon_{NH_2OH}$ and $^{18}\epsilon_{ND}$ are the respective net isotope effects expressed during oxygen incorporation from O_2 or NO_2^- into N_2O. Here we do not consider the impact of Rayleigh fractionation on the δ^{18}O-O_2 because the O_2 pool is large relative to the fraction that is consumed (<10%) and is expected to raise the δ^{18}O-O_2 less than 2‰. Substituting (4b) into (5) produces Eq. (6) (Table 2), which includes both SP values and oxygen isotopic signatures.

The best-fit values of the parameters SP_{NH_2OH}, SP_{ND}, $^{18}\epsilon_{NH_2OH}$, and $^{18}\epsilon_{ND}$ (Table 3) were obtained by fitting Eq. (6) to our dataset ($n = 33$) using a Levenberg-Marquardt non-linear regression program (Draper and Smith, 1981).

Table 3. Isotope effects and signatures derived in this paper for N_2O production by *N. marina* C-113a. Best fit values of model parameters for Eq. (6) are given with standard deviations based on covariance estimates in Bard (1974).

parameter	value	σ	description
$^{15}\epsilon_{ND}$	56.9‰	3.8‰	N isotope effect of nitrifier-denitrification
$^{18}\epsilon_{ND}$	−8.4‰	1.4‰	O isotope effect of nitrifier-denitrification
$^{18}\epsilon_{NH_2OH}$	2.9‰	0.8‰	effective O isotope effect of NH_2OH decomposition
SP_{ND}	−10.7‰	2.9‰	site preference of N_2O from nitrifier-denitrification
SP_{NH_2OH}	36.3‰	2.4‰	site preference of N_2O from NH_2OH decomposition

Inputs were the values of SP_{total}, $\delta^{18}O\text{-}N_2O$, and $\delta^{18}O\text{-}NO_2^-$ measured for each culture, as well as the known $\delta^{18}O$ of the high-purity O_2 used in the headspaces (+25.3‰). Our estimates of the end-member SP values of N_2O are significantly lower for N_2O produced by nitrifier-denitrification (-10.7 ± 2.9‰) and higher for N_2O produced by NH_2OH decomposition (36.3 ± 2.4‰) than previous estimates (Sutka et al., 2003, 2004, 2006). A sensitivity analysis of the model reveals that the value of SP_{ND} is sensitive to the values of the isotope effects $^{18}\epsilon_{NH_2OH}$ (Supplementary Fig. S.4A and S.4C and Supplementary Table 1) and $^{18}\epsilon_{ND}$ (Supplementary Fig. S.4A) but that this sensitivity decreases in labeled water (Supplementary Fig. S.4B and S.4D and Supplementary Table 2). Drawing data from both labeled and unlabeled experiments, as we have done here, leads to acceptable levels of uncertainty (Table 3).

These results expand the range of SP values produced by ammonia oxidizers by more than 10‰. This has an impact when Eq. (4b) is used to calculate the fraction of N_2O from nitrifier-denitrification using oceanographic SP data (Charpentier et al., 2007). We used the new end-member SP values to calculate that nitrifier-denitrification by C-113a accounted for 11% to 26% of N_2O production under 20% O_2 and 43% to 87% of production under 0.5% O_2 (Table 4). The variability for a given O_2 level occurred among cultures with different cell densities; on average, the denser cultures produced relatively more N_2O by nitrifier-denitrification at low-O_2 and less at high-O_2 concentrations (also see Fig. 5).

Our estimated values of $^{18}\epsilon_{ND}$ and $^{18}\epsilon_{NH_2OH}$ were -8.4 ± 1.4‰ and $+2.9 \pm 0.8$‰, respectively. This means that N_2O produced via nitrifier-denitrification was enriched in ^{18}O by 8.4‰ relative to the NO_2^-, and N_2O produced from NH_2OH was depleted in ^{18}O by 2.9‰ relative to O_2. The ^{18}O enrichment from nitrifier-denitrification is most likely the result of a combination of kinetic and branching isotope effects. There are few published estimates of these isotope effects that we can compare with our model results. Work on the heterotrophic denitrifier *Pseudomonas aureofaciens* indicates that the branching oxygen isotope effect of NO_2^- reduction is approximately 15‰ (Casciotti et al., 2007). However, it is not known whether the same isotope effect applies to nitrifier-denitrification or if there is also a kinetic isotope effect that influences the $\delta^{18}O\text{-}N_2O$. Recent work has also addressed the isotope effects for oxygen atom incorporation by C-113a (Casciotti et al., 2010), but was not able to separate fractionation during O_2 and H_2O incorporation.

Equations (5) and (6) assume that the oxygen atoms in N_2O produced by NH_2OH decomposition come only from O_2. If a fraction of this oxygen actually comes from H_2O, then the model value of $^{18}\epsilon_{NH_2OH}$ reported in Table 3 could be too high for data from experiments in unlabeled H_2O ($\delta^{18}O\text{-}H_2O < \delta^{18}O\text{-}O_2$) and too low for data from labeled H_2O ($\delta^{18}O\text{-}H_2O > \delta^{18}O\text{-}O_2$). However, this structure was not apparent in the residuals of $^{18}\epsilon_{NH_2OH}$ from labeled vs. unlabeled experiments. When a parameter for oxygen-exchange between H_2O and NH_2OH was included in Eq. (6), we were unable to resolve it with the present data set. However, if an exchange term is included in Eq. (6) so that 20% of the oxygen atoms in N_2O produced by NH_2OH decomposition are from H_2O, then using the values of SP_{NH_2OH}, SP_{ND}, and $^{18}\epsilon_{ND}$ from Table 3 and values of SP_{total}, $\delta^{18}O\text{-}N_2O_{total}$, $\delta^{18}O\text{-}NO_2^-$, and $\delta^{18}O\text{-}O_2$ from Supplementary Tables 1 and 2, estimates of $^{18}\epsilon_{NH_2OH}$ would decrease to −3.7‰ in unlabeled water and increase to 6.7‰ in labeled water if we assume that the oxygen atoms from water are incorporated without any isotope effect. However, 20% exchange is an extreme case and available evidence does not support significant exchange of oxygen atoms between NH_2OH and water during ammonia oxidation (Casciotti et al., 2010; Hollocher et al., 1981; Dua et al., 1979). Additional experiments in ^{18}O-labeled water could shed light on the issue of oxygen exchange.

The $\delta^{18}O$ and SP signatures of the N_2O in these experiments covaried (Fig. 5). The covariation depended on the $\delta^{18}O$ of the H_2O in the media: the slope of the linear regression of SP and $\delta^{18}O\text{-}N_2O$ was negative (-0.904 ± 0.087) for experiments performed in ^{18}O-enriched H_2O (+40‰) and positive (0.152 ± 0.044) for experiments in unlabeled H_2O (−5‰) (Fig. 5). Our model provides an explanation for the covariation between SP and $\delta^{18}O\text{-}N_2O$ because it describes mixing between two N_2O sources with distinct SP values and different proportions of oxygen from O_2 and H_2O. According to Eq. (6), the sign and magnitude of the regression slope will depend upon the difference between $\delta^{18}O\text{-}O_2$ and $\delta^{18}O\text{-}H_2O$.

Table 4. The fraction of N_2O produced by nitrifier-denitrification (F_{ND}) calculated using measured SP values, Eq. (4b), and the best fit values for SP_{ND} and SP_{NH_2OH} in Table 3.

density (cells/ml^{-1})	20% O_2	2% O_2	0.5% O_2
2×10^2	0.26 ± 0.06, $n=5$	0.38 ± 0.04, $n=5$	0.43 ± 0.09, $n=4$
2.1×10^4	0.19 ± 0.03, $n=5$	0.18 ± 0.04, $n=5$	0.48 ± 0.11, $n=5$
2×10^5	0.11 ± 0.03, $n=6$		0.58 ± 0.11, $n=6$
1.5×10^6			0.87 ± 0.09, $n=5$

Positive correlations between δ^{18}O-N_2O and SP observed in environmental data have been interpreted as signs that N_2O consumption by denitrification is an important N_2O cycling process in the system under scrutiny (Koba et al., 2009; Yoshida and Toyoda, 2000; Popp et al., 2002; Toyoda et al., 2002; Schmidt et al., 2004). Indeed, there is experimental evidence demonstrating that progressive consumption of N_2O by denitrifier cultures results in a simultaneous increase in both SP and δ^{18}O-N_2O (Ostrom et al., 2007). The theoretical basis for this behavior is the fact that the N-O bonds formed by the heavier nitrogen and oxygen isotopes have lower zero-point energies and are therefore more resistant to being broken than bonds between the lighter isotopes (Yung and Miller, 1997; Toyoda et al., 2002). As a result, decomposition of a symmetrical O-N-N-O intermediate during N_2O formation and also cleavage of the N-O bond during N_2O reduction to N_2 will produce N_2O with positively correlated δ^{18}O and SP values.

Our work demonstrates that SP and δ^{18}O-N_2O can also covary as a result of N_2O production by nitrification, without invoking N_2O consumption by heterotrophic denitrifiers. The sign and magnitude of the correlation depends on the difference between the δ^{18}O of the O_2 and the H_2O that contribute oxygen atoms to the N_2O. In contrast to this study, where we manipulated δ^{18}O-H_2O, there is little natural variation in δ^{18}O-H_2O in the open ocean but much larger variation in δ^{18}O-O_2 as a result of isotopic fractionation associated with respiratory O_2 consumption (Kroopnick and Craig, 1976; Bender, 1990; Levine et al., 2009). According to model Eq. (6), we would expect the slopes of the δ^{18}O-N_2O:SP regressions (such as those in Fig. 5) to increase as δ^{18}O-O_2 rises relative to δ^{18}O-H_2O (or δ^{18}O-NO_2^-). Nitrification may therefore influence the δ^{18}O-N_2O:SP dynamics in the oxycline in two opposing ways : 1) a drop in O_2 concentration may promote nitrifier-denitrification and thus the incorporation of low-δ^{18}O oxygen atoms from H_2O into low-SP N_2O, and 2) respiratory O_2 consumption increases the δ^{18}O of the remaining O_2 pool, raising the δ^{18}O of the N_2O produced by NH_2OH decomposition as well as nitrifier-denitrification. In the future, the combined use of SP, δ^{18}O-N_2O, and δ^{18}O-O_2 may be used to resolve these effects. An important unknown that remains in the marine N_2O isotope biogeochemistry is whether archaeal ammonia oxidizers also produce N_2O and if so, what their impact is on the N_2O budget and the isotopic signatures of N_2O in the ocean.

4 Conclusions

As shown previously, culturing conditions influence N_2O yields from ammonia-oxidizing bacteria. However, the yields observed in this study were much lower than those obtained in previous culture-based measurements, and they did not increase as dramatically at low oxygen concentrations except at high cell densities. These results are in line with modeling- and incubation-based oceanographic estimates of N_2O yields from nitrification and may be useful in future modeling of N_2O production and distributions in the ocean. Recent work interpreting isotopic signatures of biogenic N_2O has often relied on the assumption that a direct relationship between δ^{18}O-N_2O and SP was indicative of N_2O consumption and production by denitrification. However, our work suggests that a direct relationship between these signatures may also occur as a result of nitrification, at least when the SP values vary between -10‰ and 36‰. Nitrification produces this relationship through mixing between high-SP, ^{18}O-enriched N_2O produced by NH_2OH decomposition and low-SP, ^{18}O-depleted N_2O produced by nitrifier-denitrification.

Appendix A

Calculating the position-specific $^{15}N/^{14}N$ ratios of N_2O

Data collected during continuous flow isotopic analyses of N_2O included simultaneous signal intensities (in volt-seconds) of 30, 31, 44, 45, and 46 mass/charge detectors. The delta values and site preferences reported here were calculated using the raw peak area ratios of 31/30, 45/44, and 46/44 for a reference gas injection and the eluted sample peak. Isodat software reports these raw ratios as rR 31NO/30NO, etc. For each run, sample raw ratios were referenced to the standard ratios and these

"ratios of ratios" were multiplied by the appropriate standard ratios ($^{31}R_{standard} = 0.004054063$, $^{45}R_{standard} = 0.007743032$, $^{46}R_{standard} = 0.002103490$) to calculate $^{31}R_{sample}$, $^{45}R_{sample}$, and $^{46}R_{sample}$, respectively. For example,

$$^{31}R_{sample} = [rR\ 31NO/30NO_{sample}]/$$

$$[rR\ 31NO/30NO_{standard}] \times {}^{31}R_{standard}$$

The $R_{standard}$ values are the calculated ratios that the Farraday cups in the Casciotti Delta^{PLUS} isotope ratio mass spectrometer (IRMS) should detect whenever the standard gas is analyzed under normal operating conditions. They depend on the actual isotopic/isotopomeric composition of the standard gas and also how that gas is fragmented in the IRMS. To calculate these three values we used 1) values of $\delta^{15}N^{\alpha}$, $\delta^{15}N^{\beta}$, and $\delta^{18}O$ for our standard gas as measured by Sakae Toyoda and 2) The relative yields of *m/z* 30 and 31 from $^{15}N^{14}NO$ and $^{14}N^{15}NO$ when these isotopomers are analyzed in the Casciotti IRMS (see Appendix B for details).

$^{31}R_{sample}$, $^{45}R_{sample}$, and $^{46}R_{sample}$ values are then entered into the following equations:

$$^{31}R = ((1-\gamma)^{15}R^{\alpha} + \kappa^{15}R^{\beta} + {}^{15}R^{\alpha}{}^{15}R^{\beta} + {}^{17}R(1 + \gamma^{15}R^{\alpha} + (1-\kappa)^{15}R^{\beta}))/(1 + \gamma^{15}R^{\alpha} + (1-\kappa)^{15}R^{\beta})$$

$$^{45}R = {}^{15}R^{\alpha} + {}^{15}R^{\beta} + {}^{17}R$$

$$^{46}R = ({}^{15}R^{\alpha} + {}^{15}R^{\beta})^{17}R + {}^{18}R + {}^{15}R^{\alpha}{}^{15}R^{\beta}$$

$$^{17}R/0.0003799 = (^{18}R/0.0020052)^{0.516}$$

where γ and κ are the yields of the scrambled fragment ions from $^{14}N^{15}NO$ ($^{30}NO^{+}$) and $^{15}N^{14}NO$ ($^{31}NO^{+}$), respectively (see Appendix B). The four equations above can be evaluated with a nonlinear equation solver to obtain values for $^{15}R^{\alpha}$, $^{15}R^{\beta}$, ^{17}R, and ^{18}R for each sample.

Appendix B

Calculating *m/z* 30 and 31 yield coefficients

When N_2O is introduced into the ion source of the mass spectrometer, NO^{+} fragment ions are produced. While most of these ions contain N from the α position, a small amount of "scrambling" occurs, yielding NO^{+} ions containing the β N. Accurate measurements of $^{15}R^{\alpha}$ and $^{15}R^{\beta}$ require quantification of the scrambling behavior for the mass spectrometer under standard operating conditions.

Westley et al. (2007) use six separate coefficients to describe the $^{30}NO^{+}$ and $^{31}NO^{+}$ fragmentation behaviors of the $^{14}N^{15}NO$, $^{15}N^{14}NO$, and $^{15}N^{15}NO$ molecules. We followed their recommendation and performed mixing analyses using purified $^{14}N^{15}NO$, $^{15}N^{14}NO$, and $^{15}N^{15}NO$ gases from ICON (Summit, N. J.) to investigate the fragmentation behavior of individual isotopologues in our mass spectrometer (see supplementary material). We also compared this approach to the results of a simpler approach using two scrambling coefficients, γ and κ, to describe the relative production of $^{30}NO^{+}$ ions from $^{14}N^{15}NO$ and $^{31}NO^{+}$ ions from $^{15}N^{14}NO$, respectively. These coefficients were used in the system of equations that convert ^{31}R, ^{45}R, and ^{46}R to $^{15}R^{\alpha}$, $^{15}R^{\beta}$, ^{17}R, and ^{18}R for each sample (see Appendix A for the full set of equations).

We calculated γ and κ using a series of dual inlet measurements of two sample gases with known isotope and isotopomer ratios referenced to a standard gas that also has a known isotopic composition. In this case, the sample gases were from the laboratories of K. Koba (Tokyo University of Agriculture and Technology) and N. Ostrom (Michigan State University), and the standard gas was the reference gas from the Casciotti lab (WHOI). These three N_2O reference gases were all calibrated by S. Toyoda (Tokyo Institute of Technology).

For each sample gas the "measured" value of $[rR\ 31NO/30NO_{sample}]/[rR\ 31NO/30NO_{standard}]$ was determined by averaging the results of a series of 10-cycle dual inlet analyses on the Casciotti IRMS. Then the "calculated" value of $[rR\ 31NO/30NO_{sample}]/[rR\ 31NO/30NO_{standard}]$ (equivalent to $^{31}R_{sample}/^{31}R_{standard}$) was obtained by inserting Toyoda's calibrated values of $^{15}R^{\alpha}$, $^{15}R^{\beta}$, ^{17}R, and ^{18}R for the sample and standard gases into the equation below and guessing values of γ and κ:

$$^{31}R = ((1-\gamma)\ {}^{15}R^{\alpha} + \kappa^{15}\ R^{\beta} + {}^{15}R^{\alpha}\ {}^{15}R^{\beta} + {}^{17}R\ (1 + \gamma\ {}^{15}R^{\alpha} + (1-\kappa)\ {}^{15}R^{\beta}))/(1 + \gamma\ {}^{15}R^{\alpha} + (1-\kappa)\ {}^{15}R^{\beta})$$

The problem is one of optimization where the object is to vary γ and κ until the calculated values of $^{31}R_{sample}$ / $^{31}R_{standard}$ are as close as possible to the measured $[rR\ 31NO/30NO_{sample}]/[rR\ 31NO/30NO_{standard}]$ for both sample gases. This two-coefficient model automatically obeys the constraint of Toyoda and Yoshida (1999) that $\delta^{15}N^{bulk} = ({}^{15}R^{\alpha} + {}^{15}R^{\beta})/2$. The optimized values obtained here are $\gamma = 0.1002$ and $\kappa = 0.0976$. These coefficients are consistent with reported values for fragment ion yields and scrambling coefficients (between 0.08–0.10) (Westley et al., 2007; Toyoda and Yoshida, 1999).

Following the alternative approach of Westley et al. (2007) we found that ionization of the $^{15}N^{14}NO$ ICON standard produced approximately one tenth as many $^{31}NO^{+}$ as the $^{14}N^{15}NO$ ICON standard (see supplementary material for data and calculations). This result is an independent confirmation of the scrambling coefficient approach described above (because $\kappa/(1-\gamma) = 0.108$) and it does not require a priori knowledge of the isotopomeric composition of the reference gas.

For the data presented in this paper, we opted to use two coefficients and assumed that the fragment ion yields of 30 and 31 sum to 1 for both $^{14}N^{15}NO$ and $^{15}N^{14}NO$. Using this approach we were able to reproduce the isotopomer ratio values of sample gases with a broad range of site preferences

(calibrated value for N. Ostrom tank = + 26.5‰ and the value measured using our approach = + 27.0‰; calibrated value of K. Koba tank = −5.4‰ and measured = −4.8‰).

Supplementary material related to this article is available online at: http://www.biogeosciences.net/7/2695/2010/ bg-7-2695-2010-supplement.pdf.

Acknowledgements. We gratefully acknowledge Sakae Toyoda for calibrating our N_2O reference gas, Robin Sutka and Nathaniel Ostrom for providing the calibrated Michigan State reference gas, and Keisuke Koba for providing the calibrated Tokyo University of Agriculture and Technology reference gas. Marian Westley kindly provided extensive details on her isotopomer intercalibration strategy. Ed Leadbetter suggested the test for heterotrophic denitrification and the high cell density N_2O measurements. Matt McIlvin helped develop the modification necessary to do large-bottle headspace analyses on the MS. Matt First and Mark Dennett provided assistance with the flow cytometer. Alyson Santoro, Cara Manning, Ed Leadbetter, and three anonymous reviewers provided suggestions that improved the manuscript immensely.

Edited by: J. Middelburg

References

Alldredge, A. L. and Cohen, Y.: Can microscale chemical patches persist in the sea?, Microelectrode study of marine snow, fecal pellets, Science, 235, 689–691, 1987.

Andersson, K. K. and Hooper, A. B.: O_2 and H_2O are each sources of one O in NO_2^- produced from NH_3 by *Nitrosomonas*: ^{15}N-NMR evidence, FEBS Lett., 164, 236–240, 1983.

Andersson, K. K., Philson, S. B., and Hooper, A. B.: ^{18}O isotope shift in ^{15}N NMR analysis of biological N-oxidations: H_2O-NO_2^- exchange in the ammonia-oxidizing bacterium *Nitrosomonas*, P. Natl. Acad. Sci., 79, 5871–5875, 1982.

Arp, D. J., Chain, P. S. G., and Klotz, M. G.: The impact of genome analyses on our understanding of ammonia-oxidizing bacteria, Annu. Rev. Microbiol., 61, 503–528, 2007.

Bard, Y.: Nonlinear parameter estimation, Academic Press, New York, 1974.

Beaumont, H. J. E., Hommes, N. G., Sayavedra-Soto, L. A., Arp, D. J., Arciero, D. M., Hooper, A. B., Westerhoff, H. V., and van Spanning, R. J. M.: Nitrite reductase of *Nitrosomonas europaea* is not essential for production of gaseous nitrogen oxides and confers tolerance to nitrite, J. Bacteriol., 184, 2557–2560, 2002.

Beaumont, H. J. E., Lens, S., Reijnders, W. N. M., Westerhoff, H. V., and van Spanning, R. J. M.: Expression of nitrite reductase in *Nitrosomonas europaea* involves NsrR, a novel nitrite-sensitive transcription repressor, Mol. Microbiol., 54, 148–158, 2004.

Beman, M. J., Arrigo, K. R., and Matson, P. A.: Agricultural runoff fuels large phytoplankton blooms in vulnerable areas of the ocean, Nature, 434, 211–214, 2005.

Bender, M. L.: The δ^{18}O of dissoved O_2 in seawater: a unique tracer of circulation and respiration in the deep sea, J. Geophys. Res.-Oceans, 95, 22243–22252, 1990.

Buchwald, C. and Casciotti, K. L.: Oxygen isotopic fractionation and exchange during bacterial nitrite oxidation, Limnol. Oceanogr., 55, 1064–1074, 2010.

Cantera, J. J. and Stein, L. Y.: Molecular diversity of nitrite reductase genes (nirK) in nitrifying bacteria, Environmental Microbiology, 9, 765–776, 2007.

Carlucci, A. F. and McNally, P. M.: Nitrification by marine bacteria in low concentrations of substrate and oxygen, Limnol. Oceanogr., 14, 736–739, 1969.

Casciotti, K. L. and Ward, B. B.: Dissimilatory nitrite reductase genes from autotrophic ammonia-oxidizing bacteria, Appl. Environ. Microb., 67, 2213–2221, 2001.

Casciotti, K. L. and Ward, B. B.: Phylogenetic analysis of nitric oxide reductase gene homologues from aerobic ammonia-oxidizing bacteria, FEMS Microbiol. Ecol., 52, 197–205, 2005.

Casciotti, K. L., Sigman, D. M., Hastings, M. G., Bohlke, J. K., and Hilkert, A.: Measurements of the oxygen isotopic composition of nitrate in seawater and freshwater using the denitrifier method, Anal. Chem., 74, 4905–4912, 2002.

Casciotti, K. L., Bohlke, J. K., McIlvin, M., Mroczkowski, S. J., and Hannon, J. E.: Oxygen isotopes in nitrite: analysis, calibration, and equilibration, Anal. Chem., 79, 2427–2436, 2007.

Casciotti, K. L., McIlvin, M., and Buchwald, C.: Oxygen isotopic exchange and fractionation during bacterial ammonia oxidation, Limnol.Oceanogr., 55, 753–762, 2010.

Charpentier, J., Farias, L., Yoshida, N., Boontanon, N., and Raimbault, P.: Nitrous oxide distribution and its origin in the central and eastern South Pacific Subtropical Gyre, Biogeosciences, 4, 729–741, 2007, http://www.biogeosciences.net/4/729/2007/.

Cline, J. D., Wisegarver, D. P., and Kelly-Hansen, K.: Nitrous oxide and vertical mixing in the equatorial Pacific during the 1982–1983 El Niño, Deep-Sea Res., 34, 857–873, 1987.

Codispoti, L. A. and Christensen, J. P.: Nitrification, denitrification and nitrous oxide cycling in the eastern tropic south Pacific Ocean, Mar. Chem., 16, 277–300, 1985.

Codispoti, L. A., Brandes, J. A., Christensen, J. P., Devol, A. H., Naqvi, S. W. A., Paerl, H. W., and Yoshinari, T.: The oceanic fixed nitrogen and nitrous oxide budgets: moving targets as we enter the anthropocene?, Sci. Mar., 65, 85–105, 2001.

Cohen, Y. and Gordon, L. I.: Nitrous oxide in the oxygen minimum of the eastern tropical North Pacific: evidence for its consumption during denitrification and possible mechanisms for its production, Deep-Sea Res., 25, 509–524, 1978.

Cohen, Y. and Gordon, L. I.: Nitrous oxide production in the ocean, J. Geophys. Res., 84, 347–353, 1979.

Draper, N. R. and Smith, H.: Applied regression analysis, Wiley, New York, 2, 1981.

Dua, R. D., Bhandari, B., and Nicholas, D. J. D.: Stable isotope studies on the oxidation of ammonia to hydroxylamine by *Nitrosomonas europaea*, FEBS Lett., 106, 401–404, 1979.

Elkins, J. W., Wofsy, S., McElroy, M. B., Kolb, C. E., and Kaplan, W. A.: Aquatic sources and sinks for nitrous oxide, Nature, 275, 602–606, 1978.

Fuhrman, J. A. and Capone, D. G.: Possible biogeochemical consequences of ocean fertilization, Limnol. Oceanogr., 36, 1951–1959, 1991.

Fulweiler, R. W., Nixon, S. W., Buckley, B. A., and Granger, S. L.: Reversal of the net dinitrogen gas flux in coastal marine sed-

iments, Nature, 448, 180–181, 2007.

Galloway, J. N., Schlesinger, W. H., Levy II, H., Michaels, A., and Schnoor, J. L.: Nitrogen fixation: anthropogenic enhancement-environmental response, Global Biogeochem. Cy., 9, 235–252, 1995.

Goreau, T. J., Kaplan, W. A., Wofsy, S. C., McElroy, M. B., Valois, F. W., and Watson, S. W.: Production of NO_2^- and N_2O by nitrifying bacteria at reduced concentrations of oxygen, Appl. Environ. Microb., 40, 526–532, 1980.

Hallam, S. J., Mincer, T. J., Schleper, C., Preston, C. M., Roberts, K., Richardson, P. M., and DeLong, E. F.: Pathways of carbon assimilation and ammonia oxidation suggested by environmental genomic analyses of marine *Crenarchaeota*, PLoS Biol., 4, 521–536, 2006.

Hashimoto, L. K., Kaplan, W. A., Wofsy, S. C., and McElroy, M. B.: Transformations of fixed nitrogen and N_2O in the Cariaco Trench, Deep-Sea Res., 30, 575–590, 1983.

Helder, W. and de Vries, R. T. P.: Estuarine nitrite maxima and nitrifying bacteria (EMS-Dollard estuary), Neth J. Sea Res., 17, 1–18, 1983.

Hollocher, T. C., Tate, M. E., and Nicholas, D. J. D.: Oxidation of ammonia by *Nitrosomonas europaea*, J. Biol. Chem., 256, 10834–10836, 1981.

Hooper, A. B. and Terry, K. R.: Hydroxylamine oxidoreductase of *Nitrosomonas* production of nitric oxide from hydroxylamine, BBA.-Bioenergetics, 571, 12–20, 1979.

Ignarro, L. J., Fukuto, J. M., Griscavage, J. M., and Rogers, N. E.: Oxidation of nitric oxide in aqueous solution to nitrite but not nitrate: comparison with enzymatically formed nitric oxide from L-arginine, P. Natl. Acad. Sci., 90, 8103–8107, 1993.

IPCC: Climate Change 2007: The Physical Science Basis, Cambridge University Press, New York, NY, USA, 2007.

Jin, X. and Gruber, N.: Offsetting the radiative benefit of ocean iron fertilization by enhancing N_2O emissions, Geophys. Res. Lett., 30, 1–4, 2003.

Jorgensen, K. S., Jensen, H. B., and Sorensen, J.: Nitrous oxide production from nitrification and denitrification in marine sediment at low oxygen concentrations, Can. J. Microbiol., 30, 1073–1078, 1984.

Knowles, R., Lean, D. R. S., and Chan, Y. K.: Nitrous oxide concentrations in lakes: variations with depth and time, Limnol. Oceanogr., 26, 855–866, 1981.

Koba, K., Osaka, K., Tobari, Y., Toyoda, S., Ohte, N., Katsuyama, M., Suzuki, N., Itoh, M., Yamagishi, H., Kawasaki, M., Kim, S. J., Yoshida, N., and Nakajima, T.: Biogeochemistry of nitrous oxide in groundwater in a forested ecosystem elucidated by nitrous oxide isotopomer measurements, Geochim. Cosmochim. Ac., 73, 3115–3133, 2009.

Kool, D. M., Wrage, N., Oenema, O., Dolfing, J., and van Groenigen, J. W.: Oxygen exchange between (de)nitrification intermediates and H_2O and its implications for source determination of NO_3^- and N_2O: a review, Rapid Commun. Mass Sp., 21, 3569–3578, 2007.

Kroopnick, P. and Craig, H.: Oxygen isotope fractionation in dissolved oxygen in the deep sea, Earth Planet. Sc. Lett., 32, 375–388, 1976.

Law, C. S. and Ling, R. D.: Nitrous oxide flux and response to increased iron availability in the Antarctic Circumpolar Current, Deep-Sea Res. II, 48, 2509–2527, 2001.

Levine, N. M., Bender, M. L., and Doney, S. C.: The $\delta^{18}O$ of dissoved O_2 as a tracer of mixing and respiration in the mesopelagic ocean, Global Biogeochem. Cy., 23, GB1006, doi:10.1029/2007GB003162, 2009.

Lewis, R. S. and Deen, W. M.: Kinetics of the reaction of nitric oxide with oxygen in aqueous solutions, Chem. Res. Toxicol., 7, 568–574, 1994.

Lipschultz, F., Zafiriou, O. C., Wofsy, S. C., McElroy, M. B., Valois, F. W., and Watson, S. W.: Production of NO and N_2O by soil nitrifying bacteria, Nature, 294, 641–643, 1981.

Mariotti, A., Germon, J. C., Hubert, P., Kaiser, P., Letolle, R., Tardieux, A., and Tardieux, P.: Experimental determination of nitrogen kinetic isotope fractionation: some principles; illustration for the denitrification and nitrification processes, Plant Soil, 62, 413–430, 1981.

McIlvin, M. M. and Altabet, M.: Chemical conversion of nitrate and nitrite to nitrous oxide for nitrogen and oxygen isotopic analysis in freshwater and seawater, Anal. Chem., 77, 5589–5595, 2005.

McIlvin, M. M. and Casciotti, K. L.: Automated stable isotopic analysis of dissolved nitrous oxide at natural abundance levels, Limnol. Oceanogr.- Meth., 8, 54–66, 2010.

Naqvi, S. W. A., Jayakumar, D. A., Narvekar, P. V., Naik, H., Sarma, V. V. S. S., D'Souza, W., Joseph, S., and George, M. D.: Increased marine production of N_2O due to intensifying anoxia on the Indian continental shelf, Nature, 408, 346–349, 2000.

Nevison, C., Butler, J. H., and Elkins, J. W.: Global distribution of N_2O and the ΔN_2O-AOU yield in the subsurface ocean, Global Biogeochem. Cy., 17, GB1119, doi:10.1029/2003GB002068, 2003.

Norton, J. M., Klotz, M. G., Stein, L. Y., Arp, D. J., Bottomley, P. J., Chain, P. S. G., Hauser, L. J., Land, Miriam, L., Larimer, F. W., Shin, M. W., and Starkenburg, S. R.: Complete genome sequence of *Nitrosospira multiformis*, an ammonia-oxidizing bacterium from the soil environment, Appl. Environ. Microbiol., 74, 3559–3572, 2008.

Ostrom, N. E., Russ, M. E., Popp, B., Rust, T. M., and Karl, D. M.: Mechanisms of nitrous oxide production in the subtropical North Pacific based on determinations of the isotopic abundances of nitrous oxide and di-oxygen, Chemosphere-Global Change Science, 2, 281–290, 2000.

Ostrom, N. E., Pitt, A., Ostrom, P. H., Grandy, A. S., Huizinga, K. M., and Robertson, G. P.: Isotopologue effects during N_2O reduction in soils and in pure cultures of denitrifiers, J. Geophys. Res., 112, 1–12, 2007.

Pai, S.-C. and Yang, C.-C.: Formation kinetics of the pink azo dye in the determination of nitrite in natural waters, Anal. Chim. Acta, 232, 345–349, 1990.

Payne, W. J., Riley, P. S., and Cox, C. D. J.: Separate nitrite, nitric oxide, and nitrous oxide reducing fractions from *Pseudomonas perfectomarinus*, J. Bacteriol., 106, 356–361, 1971.

Popp, B. N., Westley, M. B., Toyoda, S., Miwa, T., Dore, J. E., Yoshida, N., Rust, T. M., Sansone, F. J., Russ, M. E., Ostrom, N. E., and Ostrom, P. H.: Nitrogen and oxygen isotopomeric constraints on the origins and sea-to-air flux of N_2O in the oligotrophic subtropical North Pacific gyre, Global Biogeochem. Cy., 16, GB1064, doi:10.1029/2001GB001806, 2002.

Poth, M. and Focht, D.: ^{15}N kinetic analysis of N_2O production by *Nitrosomonas europaea*: an examination of nitrifier denitrification, Appl. Environm. Microbr., 49, 1134–1141, 1985.

Remde, A. and Conrad, R.: Production of nitric oxide in *Nitrosomonas europaea* by reduction of nitrite, Arch. Microbiol., 154, 187–191, 1990.

Ritchie, G. A. F. and Nicholas, D. J. D.: Identification of the sources of nitrous oxide produced by oxidative and reductive processes in *Nitrosomonas europaea*, Biochemi. J., 126, 1181–1191, 1972.

Rodionov, D. A., Dubchak, I. L., Arkin, A. P., Alm, E. J., and Gelfand, M. S.: Dissimilatory metabolism of nitrogen oxides in bacteria: comparative reconstruction of transcriptional networks, PLoS Computational Biology, 1, 415–431, 2005.

Schmidt, H.-L., Werner, R. A., Yoshida, N., and Well, R.: Is the isotopic composition of nitrous oxide an indicator for its origin from nitrification or denitrification? A theoretical approach from referred data and microbiological and enzyme kinetic aspects, Rapid Commun. Mass Sp., 18, 2036–2040, 2004.

Shaw, L. J., Nicol, G. W., Smith, Z., Fear, J., Prosser, J., and Baggs, E. M.: *Nitrosospira* spp. can produce nitrous oxide via a nitrifier denitrification pathway, Environ. Microbiol., 8, 214–222, 2006.

Solorzano, L.: Determination of ammonia in natural waters by the phenolhypochlorite method, Limnol. Oceanogr., 14, 799–801, 1969.

Suntharalingam, P. and Sarmiento, J. L.: Factors governing the oceanic nitrous oxide distribution: simulations with an ocean general circulation model, Global Biogeochem. Cy., 14, 429–454, 2000.

Sutka, R. L., Ostrom, N. E., Ostrom, P. H., Gandhi, H., and Breznak, J. A.: Nitrogen isotopomer site preference of N_2O produced by *Nitrosomonas europaea* and *Methylococcus capsulatus* Bath, Rapid Commun. Mass Sp., 17, 738–745, 2003.

Sutka, R. L., Ostrom, N. E., Ostrom, P. H., Gandhi, H., and Breznak, J. A.: Nitrogen isotopomer site preference of N_2O produced by *Nitrosomonas europaea* and *Methylococcus capsulatus* Bath, Rapid Commun. Mass Sp., 18, 1411–1412, 2004.

Sutka, R. L., Ostrom, N. E., Ostrom, P. H., Breznak, J. A., Gandhi, H., Pitt, A. J., and Li, F.: Distinguishing nitrous oxide production from nitrification and denitrification on the basis of isotopomer abundances, Appl. Environ. Microbr., 72, 638–644, 2006.

Toyoda, S. and Yoshida, N.: Determination of nitrogen isotopomers of nitrous oxide on a modified isotope ratio mass spectrometer, Anal. Chem., 71, 4711–4718, 1999.

Toyoda, S., Yoshida, N., Miwa, T., Matsui, Y., Yamagishi, H., and Tsunogai, U.: Production mechanism and global budget of N_2O inferred from its isotopomers in the western North Pacific, Geophys. Res. Lett., 29(3), 1037, doi:10.1029/2001GL014311., 2002.

Toyoda, S., Mutobe, H., Yamagishi, H., Yoshida, N., and Tanji, Y.: Fractionation of N_2O isotopomers during production by denitrifier, Soil Biol. Biochem., 37, 1535–1545, 2005.

Treusch, A. H., Leininger, S., Kletzin, A., Schuster, S. C., Klenk, H.-P., and Schleper, C.: Novel genes for nitrite reductase and Amo-related proteins indicate a role of uncultivated mesophilic crenarchaeota in nitrogen cycling, Environ. Microbiol., 7, 1985–1995, 2005.

Walker, C. B., de la Torre, J. R., Klotz, M. G., Pinel, N., Arp, D. J., Brochier-Armanet, C., Chain, P. S. G., Chan, P. P., Gollabgir, A., and Hemp, J.: *Nitrosopumilus maritimus* genome reveals unique mechanisms for nitrification and autotrophy in globally distributed marine crenarchaea, Proceedings of the National Academy of Science, 107, 8818–8823, 2010.

Ward, B. B., Olson, R. J., and Perry, M. J.: Microbial nitrification rates in the primary nitrite maximum off southern California, Deep-Sea Res., 29, 247–255, 1982.

Watson, S. W.: Characteristics of a marine nitrifying bacterium, *Nitrosocystis oceanus* sp. nov., Limnol. Oceanogr., 10, R274–R289, 1965.

Westley, M. B., Popp, B. N., and Rust, T. M.: The calibration of the intramolecular nitrogen isotope distribution in nitrous oxide measured by isotope ratio mass spectrometry, Rapid Commun. Mass Sp., 21, 391–405, 2007.

Wrage, N., van Groenigen, J. W., Oenema, O., and Baggs, E. M.: A novel dual-isotope labelling method for distinguishing between soil sources of N_2O, Rapid Commun. Mass Sp., 19, 3298–3306, 2005.

Yoshida, N.: ^{15}N-depleted N_2O as a product of nitrification, Nature, 335, 528–529, 1988.

Yoshida, N. and Toyoda, S.: Constraining the atmospheric N_2O budget from intramolecular site preference in N_2O isotopomers, Nature, 405, 330–334, 2000.

Yoshida, N., Morimoto, H., Hirano, M., Koike, I., Matsuo, S., Wada, Eitaro adn Saino, T., and Hattori, A.: Nitrification rates and ^{15}N abundances of N_2O and NO_3^- in the western North Pacific, Nature, 342, 895–897, 1989.

Yoshinari, T.: Nitrous oxide in the sea, Mar. Chem., 4, 189–202, 1976.

Yung, Y. L. and Miller, C. E.: Isotopic fractionation of stratospheric nitrous oxide, Science, 278, 1778–1780, 1997.